Journal of Advanced Research 23 (2020) 25–35

Contents lists available at ScienceDirect

Journal of Advanced Research

journal homepage: www.elsevier.com/locate/jare

TMEM16A Ca^{2+}-activated Cl^- channel inhibition ameliorates acute pancreatitis via the IP_3R/Ca^{2+}/NFκB/IL-6 signaling pathway

Qinghua Wang [a,b,1], Lichuan Bai [a,1], Shuya Luo [a], Tianyu Wang [a], Fan Yang [a], Jialin Xia [a], Hui Wang [a], Ke Ma [a], Mei Liu [a], Shuwei Wu [a], Huijie Wang [a], Shibin Guo [c], Xiaohong Sun [d], Qinghuan Xiao [a,*]

[a] Department of Ion Channel Pharmacology, School of Pharmacy, China Medical University, Shenyang 110122, China
[b] Department of Experimental Center, The Affiliated Hospital of Liaoning University of Traditional Chinese Medicine, Shenyang 110032, China
[c] Department of Gastroenterological Endoscopy, the First Affiliated Hospital of Dalian Medical University, Dalian 116011, China
[d] Department of Neurology, The Fourth Affiliated Hospital of China Medical University, Shenyang 110032, China

GRAPHICAL ABSTRACT

A positive activation loop between TMEM16A and the IP_3R/Ca^{2+}/NFκB/IL-6 pathway is important for Ca^{2+} elevation, NFκB activation and IL-6 release, and thus cooperatively promotes the pathogenesis of AP.

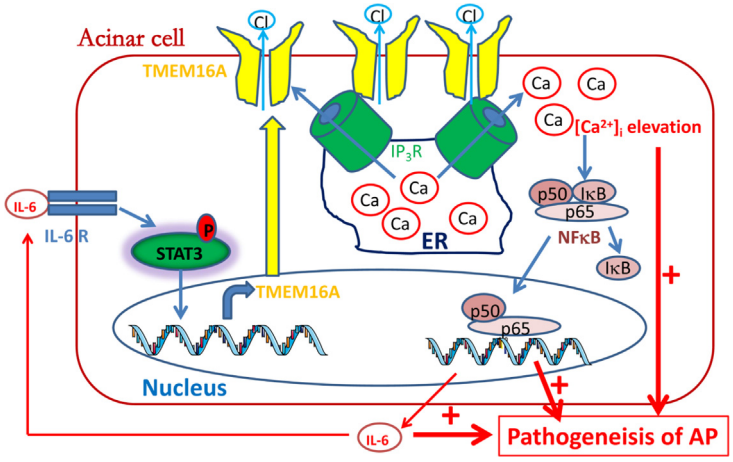

Abbreviations: AP, acute pancreatitis; T16Ainh-A01, TMEM16A inhibitor-A01; CaCCinh-A01, Ca^{2+}-activated Cl^- channel inhibitor-A01; PACs, pancreatic acinar cells; CCK, cholesystokinin; IP_3R, inositol 1,4,5-trisphosphate receptor; ER, endoplasmic reticulum; IL-6, interleukin 6; IL-6R, interleukin 6 receptor; STAT3, signal transducers and activators of transcription 3; NFκB, nuclear factor-κB; shRNAs, short hairpin RNAs; FBS, fetal bovine serum; EGFP, green fluorescent protein; RIPA, radio immunoprecipitation assay; SDS-PAGE, sodium dodecyl sulfate polyacrylamide gel electrophoresis; ELISA, enzyme-linked immunosorbent assay; Tris, tris(hydroxymethyl)aminomethane; NP-40, Nonidet P-40; HEPES, N-2-hydroxyethil-piperazine-N'-2-ethanesulfonic acid; EDTA, ethylenediaminetetraacetic acid; EGTA, ethylene glycol-bis(2-aminoethyl ether)-N,N,N', N'-tetraacetic acid; NMDG, N-methyl-D-glucamine; BAPTA-AM, 1,2-bis(2-aminophenoxy)ethane-N,N,N′,N′-tetraacetic acid-acetyloxymethyl ester; WT, wild type; EGF, epidermal growth factor; EGFR, epidermal growth factor receptor; CFBE, cystic fibrosis bronchial epithelial.

Peer review under responsibility of Cairo University.

* Corresponding author at: Department of Ion Channel Pharmacology, School of Pharmacy, China Medical University, No. 77 Puhe Road, Shenyang North New Area, Shenyang 110122, China.

E-mail address: qinghuanxiao12345@163.com (Q. Xiao).

[1] Q.W. and L.B. contributed equally to this work.

https://doi.org/10.1016/j.jare.2020.01.006
2090-1232/

ARTICLE INFO

Article history:
Received 24 November 2019
Revised 14 January 2020
Accepted 18 January 2020
Available online 21 January 2020

Keywords:
TMEM16A
Inositol 1,4,5-trisphosphate receptor
Acute pancreatitis
NFκB
Interleukin-6

ABSTRACT

TMEM16A Ca^{2+}-activated Cl^- channels are expressed in pancreatic acinar cells and participate in inflammation-associated diseases. Whether TMEM16A contributes to the pathogenesis of acute pancreatitis (AP) remains unknown. Here, we found that increased TMEM16A expression in the pancreatic tissue was correlated with the interleukin-6 (IL-6) level in the pancreatic tissue and in the serum of a cerulein-induced AP mouse model. IL-6 treatment promoted TMEM16A expression in AR42J pancreatic acinar cells via the IL-6 receptor (IL-6R)/signal transducers and activators of transcription 3 (STAT3) signaling pathway. In addition, TMEM16A was co-immunoprecipitated with the inositol 1,4,5-trisphosphate receptor (IP_3R) and was activated by IP_3R-mediated Ca^{2+} release. TMEM16A inhibition reduced the IP_3R-mediated Ca^{2+} release induced by cerulein. Furthermore, TMEM16A overexpression activated nuclear factor-κB (NFκB) and increased IL-6 release by increasing intracellular Ca^{2+}. TMEM16A knockdown by shRNAs reduced the cerulein-induced NFκB activation by Ca^{2+}. TMEM16A inhibitors inhibited NFκB activation by decreasing channel activity and reducing TMEM16A protein levels in AR42J cells, and it ameliorated pancreatic damage in cerulein-induced AP mice. This study identifies a novel mechanism underlying the pathogenesis of AP by which IL-6 promotes TMEM16A expression via IL-6R/STAT3 signaling activation, and TMEM16A overexpression increases IL-6 secretion via IP_3R/Ca^{2+}/NFκB signaling activation in pancreatic acinar cells. TMEM16A inhibition may be a new potential strategy for treating AP.

Introduction

Acute pancreatitis (AP) is an inflammatory disease with a severity ranging from mild edema in the pancreas to severe inflammation with systemic involvement [1]. The incidence of AP is approximately 13–45 cases/100,000 people and is increasing worldwide [2]. No therapeutic agents that inhibit the progression of AP are currently available [3]. Therefore, it is urgent to develop a novel agent that can ameliorate AP.

TMEM16A (anoctamin 1) is a Ca^{2+}-activated Cl^- channel that participates in various physiological functions ranging from the secretion of epithelial fluid and the contraction of skeletal and smooth muscles to blood pressure control [4–6]. Recent studies have revealed that TMEM16A expression is upregulated in many diseases including cancer, hypertension, and cystic fibrosis [6–8]. In addition, TMEM16A overexpression is found in many inflammation-associated diseases such as asthma, cystic fibrosis, and chronic rhinosinusitis [8–11]. TMEM16A inhibition by its inhibitors such as T16Ainh-A01 (TMEM16A inhibitor-A01) and CaCCinh-A01 (Ca^{2+}-activated Cl^- channel inhibitor-A01) (the structure of the inhibitors is shown in Fig. S1) blocks the development of cancer and inflammation [8,9]. Therefore, TMEM16A inhibitors may be promising for treating TMEM16A overexpression-associated inflammatory diseases.

TMEM16A has been immunohistochemically detected in the pancreatic tissues [12], including in acinar cells [13,14], islets [15], and duct cells [16], as well as in pancreatic cancer cells [17]. TMEM16A mediates Ca^{2+}-activated Cl^- and HCO_3^- transport in pancreatic acinar cells (PACs) [18,19]. TMEM16A-mediated Cl^- secretion may function as a main driving force for secreting fluids in PACs [14]. TMEM16A-mediated HCO_3^- transport in PACs is important for luminal pH regulation, and TMME16A inhibition increases luminal acidosis in AP induced by supramaximal cholesystokinin (CCK) treatment [19]. However, although TMEM16A has been implicated in luminal pH regulation in AP, no studies have investigated whether TMEM16A contributes to the pathogenesis of AP.

Sustained intracellular Ca^{2+} elevation in PACs activates trypsinogen, causes mitochondrial dysfunction, induces NFκB activation, and has been recognized as a critical mechanism underlying the pathogenesis of AP [3,20]. Many known stimuli that induce AP, such as alcohol, CCK hyperstimulation, and bile acids, elicit sustained Ca^{2+} elevation in PACs by activating the inositol 1,4,5-trisphosphate receptor (IP_3R) Ca^{2+} channel in the endoplasmic reticulum (ER) [20]. TMEM16A binds directly to IP_3R and is activated by IP_3R-mediated Ca^{2+} release in dorsal root ganglia cells and HeLa cells (the human epithelial cancer cells of the cervix that have been maintained in culture since 1951 and are often used in research) [21,22], though this direct interaction between TMEM16A and IP_3R is not found in cerebral artery smooth muscles [23]. In addition, several lines of evidence have shown that TMEM16A overexpression increases intracellular Ca^{2+} concentrations [17,22]. However, it is unknown whether TMEM16A is involved in the pathogenesis of AP by increasing IP_3R-mediated Ca^{2+} elevation.

Here, we studied the mechanism of TMEM16A channels in AP induced by cerulein, a CCK analog that is experimentally used for creating AP models. Both animal and cellular studies showed that TMEM16A expression was upregulated in PACs. TMEM16A upregulation was caused by interleukin 6 (IL-6)/IL-6 receptor (IL-6R)/signal transducers and activators of transcription 3 (STAT3) signaling activation in AR42J cells. TMEM16A overexpression activated nuclear factor-κB (NFκB) and increased IL-6 secretion. TMEM16A inhibition by short hairpin RNAs (shRNAs) to silence the targeted gene or by inhibitors to block channel currents reduced the TMEM16A currents, inhibited IP_3R-mediated Ca^{2+} release, and blocked NFκB activation and IL-6 secretion in AR42J cells following cerulein treatment. TMEM16A inhibitors ameliorated pancreatic damage in cerulein-induced AP mice. Our findings suggest that TMEM16A promotes the pathogenesis of AP via activation of the IP_3R/Ca^{2+}/NFκB/IL-6 pathway, and TMEM16A inhibition may be a promising strategy for the treatment of AP.

Materials and methods

Animals

The Animal Ethics Committee of Liaoning University of Traditional Chinese Medicine approved the experimental protocol for animal use (No. 2019YS (DW)-024-01). All animal experiments were conducted in accordance with the National Institutes of Health Guide for the Care and Use of Laboratory Animals. C57BL/6N mice (male, 8–10 weeks old, weighing 20–24 g) were housed at 25 °C with 3.3. water and food *ad libitum*.

Mouse model of cerulein-induced AP

The mouse model of AP was created by a series of 7 intraperitoneal injections of supramaximal cerulein (50 μg/kg; Sigma-Aldrich, USA) spaced one hour apart. To investigate the time course of TMEM16A expression in AP mice, 24 mice were randomly assigned to 4 groups (n = 6 per group) based on sacrifice time at 0, 6, 12, and 24 h after the last cerulein injection. To study the *in vivo* effect of T16Ainh-A01, 18 mice were randomly assigned to 3 groups (n = 6 per group): the control group, the AP group, and the AP + T16Ainh-A01 group. For the AP + T16Ainh-A01 group, AP mice received intraperitoneal injection of T16Ainh-A01 (1 mg/kg) 30 min prior to the first cerulein injection. Equal volumes of normal saline were injected in control mice. The mice were sacrificed 12 h after the last cerulein injection. Blood and pancreatic tissues were collected for further analysis.

Histological examination of the pancreas

Pancreatic tissue sections (5 μm thick) were stained with hematoxylin and eosin. The severity of pancreatitis was assessed using a scoring system that evaluated four pathological parameters: edema (0–4), acinar cell necrosis (0–4), inflammation (0–4), and intrapancreatic hemorrhage (0–4) [24]. The final pathological score (range, 0–16) was determined by the summation of the score for each parameter.

Cell culture and transfection

Pancreatic acinar AR42J cells (ATCC, Manassas, USA) were cultured in RPMI 1640 medium (HyClone) supplemented with 20% fetal bovine serum (FBS) and 1% penicillin and streptomycin to prevent bacterial contamination in a humid incubator (37 °C, 5% CO_2). The cell model of AP was created by treating cells with cerulein (10 nM) for 24 h.

AR42J cells were transfected with TMEM16A-expressing plasmids in the pEGFP-N1 vector and the control empty vector [12] or with TMEM16A-shRNAs and scrambled control shRNAs in the pGPU6-EGFP vector (constructed by Shanghai GenePharma, China) using Lipofectamine 2000 (Invitrogen) according to the manufacture's protocol. The pEGFP-N1 vector and the pGPU6-EGFP vector encode enhanced green fluorescent protein (EGFP), which exhibits green fluorescence under a fluorescence microscope and can be used as a reporter to detect the transfected cells.

Western blot

For TMEM16A expression, pancreatic tissues or AR42J cells were homogenized in radio immunoprecipitation assay (RIPA) buffer (Beyotime Biotechnology, China). For NFκB/p65 (65 kD) nuclear translocation, nuclear and cytoplasmic pools were generated using the nuclear and cytoplasmic protein extraction kit (KeyGEN, China). After protein separation by sodium dodecyl sulfate polyacrylamide gel electrophoresis (SDS-PAGE) and electroblot transfer, the membranes were incubated with primary antibodies against TMEM16A (1:2,000), STAT3 (1:1,000), phosphorylated STAT3 (p-STAT3; 1:1,000), NFκB/p65 (1:1,000) or IP_3R (1:1,000) overnight at 4 °C, followed by secondary antibodies (1:10,000) at room temperature for 1 h. Bands were visualized using chemiluminescence detection agents. All primary and secondary antibodies were from Abcam Biotechnology, UK.

Enzyme-linked immunosorbent assay (ELISA)

The IL-6 levels in the AR42J cell culture medium and in the mouse serum and pancreatic tissues were determined using an IL-6 ELISA kit (AMEKO, Shanghai, China) according to the manufacturer's protocols and were detected using a microplate reader (Bio-Rad, USA).

Co-immunoprecipitation

AR42J cells were homogenized for 30 min in ice-cold RIPA lysis buffer containing 50 mM Tris(hydroxymethyl)aminome thane-HCl (Tris-HCl; pH 7.4), 150 mM NaCl, 1% Nonidet P-40 (NP-40), 0.25% sodium deoxycholate, sodium orthovanadate, ethylenediaminetetraacetic acid (EDTA) and aprotinin, a protease inhibitor that inhibits proteolysis (Absin Biotechnology, China). After centrifugation, the supernatant was incubated with anti-TMEM16A antibodies or anti-IP_3R antibodies overnight at 4 °C, followed by incubation with pre-cleaned protein A/G agarose beads (20 μl) for 2 h at 4 °C. The beads were then centrifuged at 3,000 rpm for 3 min at 4 °C, washed with lysis buffer, and resuspended in the sample buffer. The samples were then analyzed by Western blot.

Measurement of intracellular Ca^{2+}

AR42J cells were loaded with the cell-permeable fluorescent Ca^{2+} dye fluo-4- acetyloxymethyl ester (Fluo-4-AM) (2 μM, Invitrogen, USA) and 0.1% F127 (Invitrogen, USA) for 50 min at 37 °C in Hank's solution, which provided physiological pH, osmotic balance and essential inorganic ions. The cells were plated on a coverslip in Hank's solution without Ca^{2+} (containing 5 mM Ca^{2+} chelator ethylene glycol-bis(2-aminoethyl ether)-N,N,N',N'-tetraacetic acid (EGTA)). The intracellular Ca^{2+} concentration in response to cerulein (10 nM) was measured using a confocal microscope (Nikon C2 plus, Japan) (excitation wavelength, 485 nm; emission wavelength, 515 nm). Fluo-4 fluorescence signal normalized to the resting level (F/F0) was used for analysis.

Patch clamp recordings

The patch clamp technique was used to record Cl^- currents in a whole-cell configuration. A P97 puller (Sutter Instruments, CA) was used to make electrodes with resistances of ~2–4 mΩ when filled with pipette solution. The data were recorded using Clampex 10 software on a computer connected to an Axopatch 200B amplifier via a Digidata system (Molecular Devices, CA, USA). AR42J cells were voltage clamped at a holding potential of 0 mV. Voltage ramps from −100 to +100 mV were applied at an interval of 10 s. Pipette solutions contained (in mM): 146 CsCl, 2 $MgCl_2$, 0.5 EGTA and 8 HEPES (N-2-hydroxyethil-piperazine-N'-2-ethanesulfonic acid), pH 7.3, adjusted with NMDG (N-methyl-D-glucamine). External solutions contained (in mM): 144 NaCl, 4 KCl, 5 EGTA, 1 $MgCl_2$, 10 glucose, and 10 HEPES (pH 7.3). Cerulein was applied to the external solution to record Ca^{2+}-activated Cl^- currents activated by IP_3R.

Statistical analysis

Origin9 software was used for graphical presentations. Clampfit10 software was used for analyzing current traces. SPSS 13.0 software was used for statistical analyses. Student's *t*-test or one-way analysis of variance (ANOVA) was used to compare the differences between groups. Spearman correlation analysis was used to evaluate the association of TMEM16A expression with the IL-6 levels in AP mice. $P < 0.05$ was considered to be statistically significant.

Results

TMEM16A expression is upregulated in cerulein-induced AP

We examined TMEM16A expression in cerulein-induced AP mice. Histological examination showed that cerulein treatment induced pancreatic damage in the mice (Fig. 1A, B). TMEM16A expression was upregulated in the pancreatic tissue of AP mice (Fig. 1C). Consistent with the animal model of cerulein-induced AP, TMEM16A expression was upregulated in AR42J cells following cerulein treatment for 6–24 h (Fig. 1D).

TMEM16A expression correlates with IL-6 levels in cerulein-induced AP mice

It is known that IL-6 is increased in AP and contributes to the pathogenesis of AP [25,26]. We examined the IL-6 levels in the pancreatic tissue and the serum of AP mice using ELISA. The IL-6

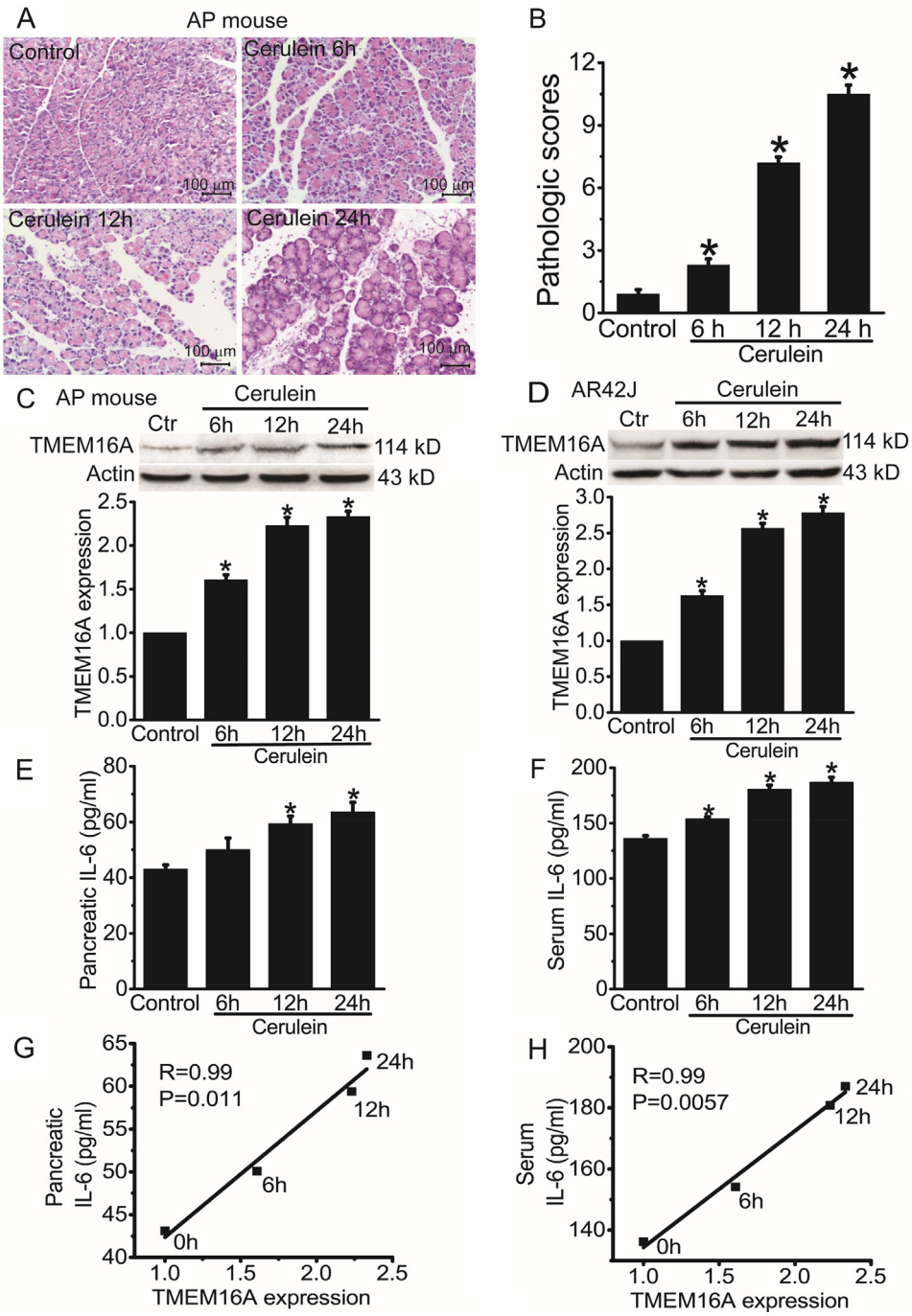

Fig. 1. TMEM16A expression was increased in cerulein-induced AP and was correlated with IL-6 expression. **A.** Representative H&E stains of pancreatic tissues of control mice and AP mice. Mice were sacrificed at 6, 12, and 24 h after the last injection of cerulein. Scale bar: 100 μm. **B.** The pathologic scores of pancreatic tissues in control mice and AP mice at 6, 12, and 24 h after cerulein treatment. n = 6 mice. *p < 0.05 vs control. **C.** Western blot analysis of TMEM16A expression in the pancreatic tissues of control mice and AP mice at 6, 12, and 24 h after the last injection of cerulein. **D.** Western blot analysis of TMEM16A expression in control AR42J cells and cells treated with 10 nM cerulein for 6–24 h. n = 3.*p < 0.05 vs control. **E, F.** ELISA results of the IL-6 levels in the pancreatic tissues (**E**) and in the serum (**F**) of control mice and AP mice at 6, 12 and 24 h after cerulein injection. n = 6. *p < 0.05 vs control. **G, H**. Correlation of TMEM16A with the IL-6 levels in the pancreatic tissues (**G**) and in the serum (**H**) of control mice and AP mice at 6, 12 and 24 h after cerulein injection. The association was analyzed using Spearman correlation analysis.

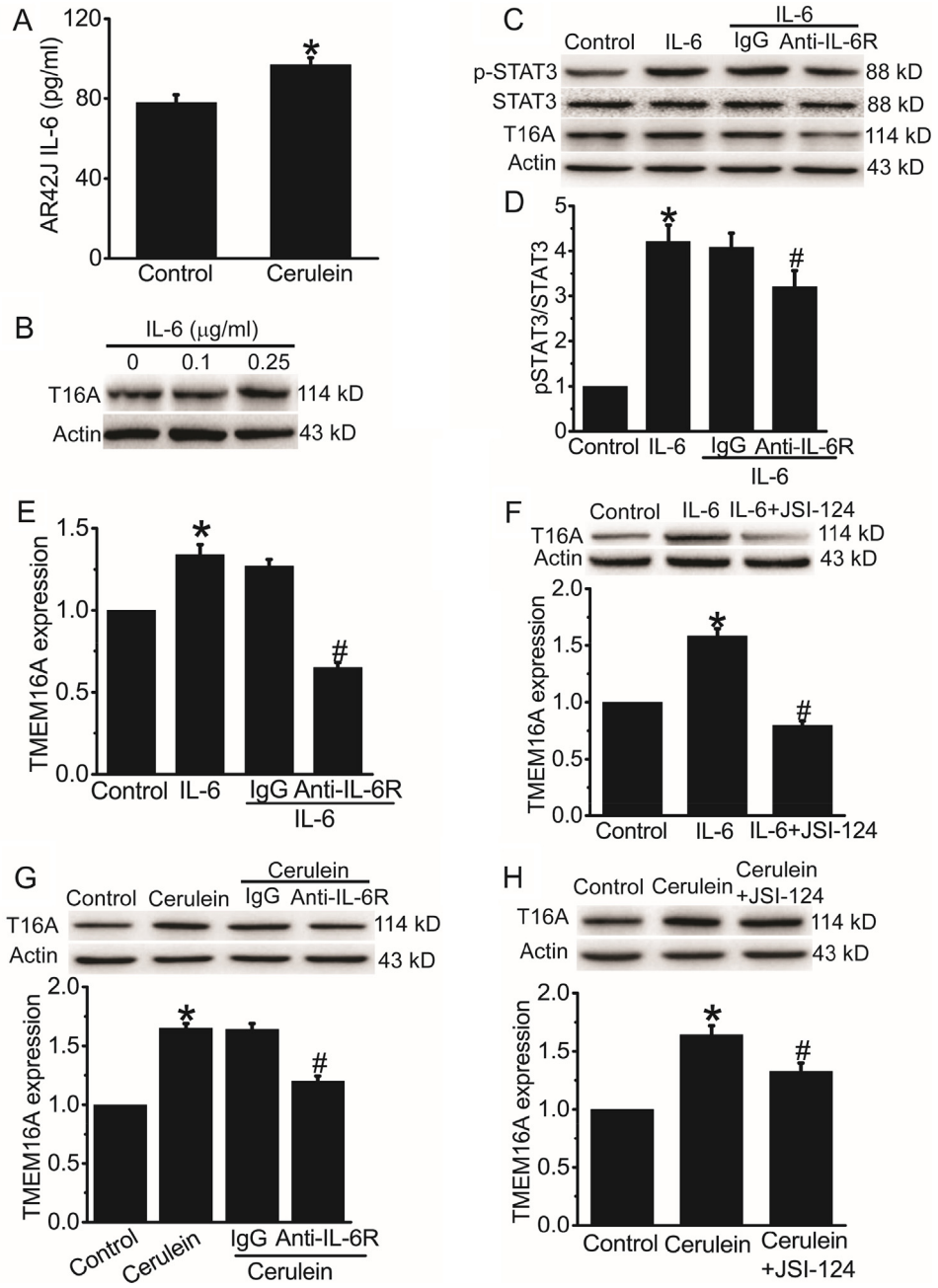

Fig. 2. IL-6 increased TMEM16A expression via the IL-6R/STAT3 signaling pathway in AR42J cells. **A**. ELISA results of the IL-6 levels in the culture medium in control AR42J cells and in cerulein-treated cells. n = 6.*p < 0.05 vs control. **B**. Western blot analysis of TMEM16A expression in AR42J cells treated with different concentrations of IL-6 (0–0.25 μg/ml) for 24 h. **C**. Western blot analysis of the expression of p-STAT3, STAT3, and TMEM16A in AR42J cells treated with 0.25 μg/ml IL-6 for 24 h. **D. E**. Quantification results of pSTAT3 (**D**) and TMEM16A (**E**) expression in C. n = 3.*p < 0.05 vs control; #p < 0.05 vs IgG. **F**. Western blot results of TMEM16A expression in control AR42J cells and cells treated with 0.25 μg/ml IL-6 for 24 in the presence or absence of the STAT3 inhibitor JSI-124 (1 μM). n = 3.*p < 0.05 vs control; #p < 0.05 vs IL-6 alone. **G. H**. Western blot results of TMEM16A expression in control AR42J cells and cerulein-treated cells in the presence or absence of antibodies against IL-6R (1 μg/ml) (**G**) or JSI-124 (1 μM) (**H**). IgG was used as control for IL-6R antibodies. n = 3.*p < 0.05 vs control; #p < 0.05 vs IgG (**G**) or cerulein alone (**H**).

levels in the pancreatic tissues and in the serum were increased in AP mice 6–24 h after cerulein injection (Fig. 1E, F). The amount of TMEM16A protein was significantly correlated with IL-6 levels in the pancreatic tissues (r = 0.99, $p = 0.011$; Fig. 1G) and in the serum (r = 0.99, $p = 0.0057$; Fig. 1F), suggesting that IL-6 may promote TMEM16A expression in AP.

IL-6 promotes TMEM16A expression via the IL-6R/STAT3 pathway in cerulein-induced AP

The ELISA results confirmed that the IL-6 concentration in the culture medium was significantly increased after cerulein treatment for 24 h (Fig. 2A), suggesting that IL-6 secretion was

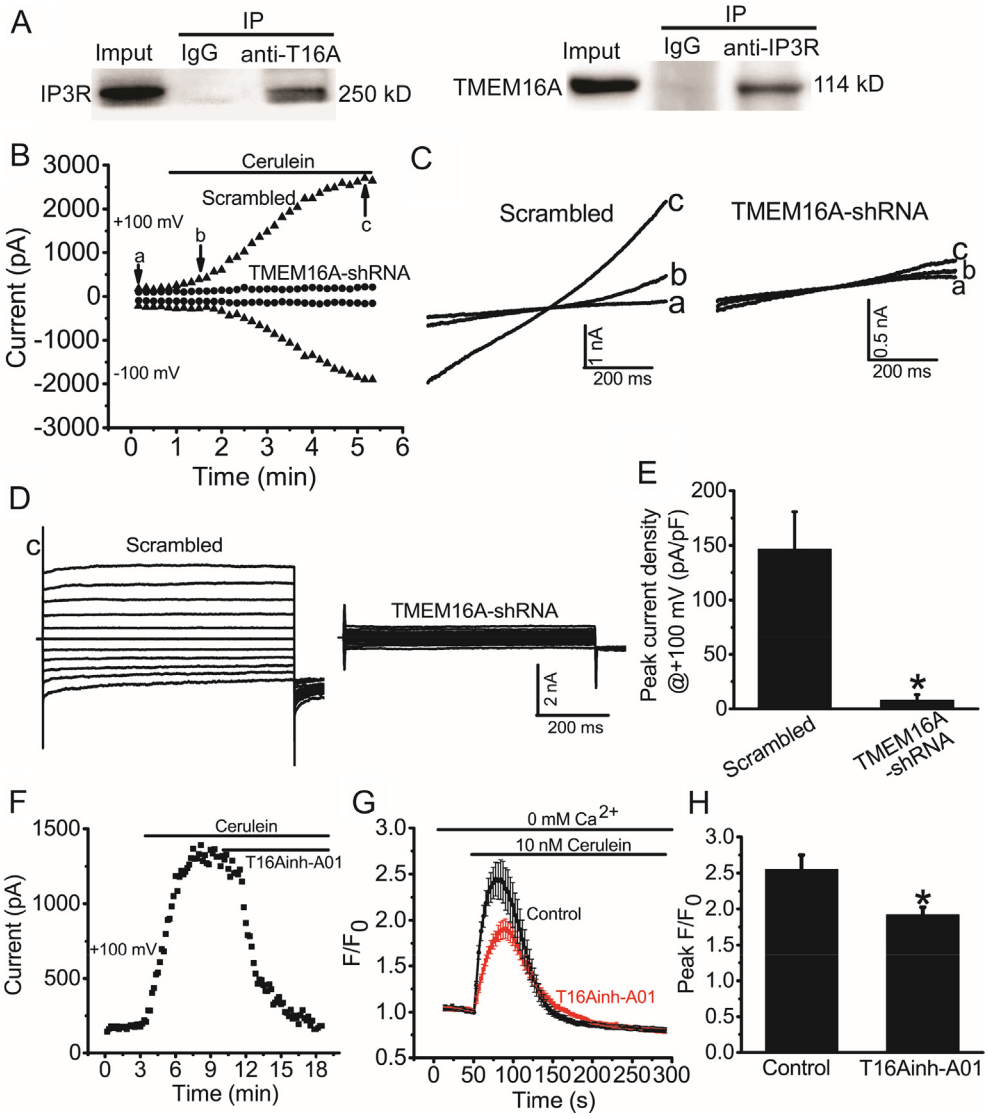

Fig. 3. TMEM16A and IP_3R activated each other in AR42J cells. **A**. Immunoprecipitation of IP_3R by antibodies against TMEM16A (anti-T16A, left) and of TMEM16A by antibodies against IP_3R (right) from lysates of AR42J cells. IgG was used as control. **B**. The time course of activation of Cl^- currents by cerulein in AR42J cells transfected with scrambled shRNAs or TMEM16A-shRNAs. Cells were recorded with 750-ms voltage ramps from − 100 to + 100 mV at an interval of 10 s. The external solution contained no Ca^{2+}. Currents at −100 mV and + 100 mV are shown. Bottom trace: the representative currents recorded before (**a**) and after (**b**) cerulein application and at the peak current (**c**). **C**. The representative currents at the time points **a**, **b**, **c** in B. **D**. The representative current at **c** recorded with a step voltage pulse from a holding potential of 0 mV to potentials between −100 mV and + 100 mV in 20 mV increments for 750 ms. **E**. Mean peak current densities at + 100 mV for cells treated with scrambled shRNA or TMEM16A-shRNA, as recorded in (**B**). n = 3–4. *p < 0.05 vs scrambled shRNA. **F**. The time course of cerulein-induced Cl^- currents inhibited by T16Ainh-A01 (20 μM) in AR42J cells. **G**. Mean Fluo-4 intensity changes (F/F0) in AR42J cells in the presence or absence of T16Ainh-A01 (20 μM). Cerulein (10 nM) was applied to induce Ca^{2+} release from IP_3R. Cells were treated with T16Ainh-A01 30 min before cerulein application. **H**. Quantification of the amplitude of the curve of Fluo-4 intensity changes (F/F0). n = 10–12 cells. *p < 0.05 vs control.

increased in the AR42J cell model of AP. IL-6 (0.25 μg/ml) treatment increased TMEM16A expression in AR42J cells (Fig. 2B). Antibodies against IL-6 receptor (anti-IL-6R) reduced IL-6-induced STAT3 activation and TMEM16A upregulation in AR42J cells (Fig. 2C-E). The STAT3 inhibitor JSI-124 inhibited IL-6-induced TMEM16A upregulation in AR42J cells (Fig. 2F). IL-6R antibodies and JSI-124 significantly inhibited cerulein-induced TMEM16A upregulation in AR42J cells (Fig. 2G, H). These findings suggested that increased IL-6 secretion from acinar cells after cerulein treatment promoted TMEM16A expression via IL-6R/STAT3 signaling activation.

TMEM16A channels and IP_3R activate each other in AR42J cells

We performed co-immunoprecipitation experiments to investigate whether TMEM16A and IP_3R directly bind to each other in AR42J cells. The co-immunoprecipitation results showed that TMEM16A directly interacted with IP_3R in AR42J cells (Fig. 3A). We then investigated whether IP_3R-mediated Ca^{2+} release activated TMEM16A Cl^- currents in AR42J cells by acute application of cerulein. Under the condition of "0" Ca^{2+} extracellular solution to exclude the possible effect of Ca^{2+} influx, whole-cell Cl^- currents in AR42J cells were gradually activated after the application of cerulein. The currents activated by cerulein exhibited outward rectification at the beginning of cerulein application and showed liner voltage-current relationships when currents were maximally activated, exhibiting the characteristic feature of TMEM16A currents (Fig. 3B-D). Cerulein-induced Cl^- currents were significantly reduced by TMEM16A-shRNA treatment (Fig. 3B-E). The TMEM16A inhibitor T16Ainh-A01 inhibited cerulein-induced Cl^- currents in AR42J cells (Fig. 3F). Furthermore, T16Ainh-A01 inhibited the

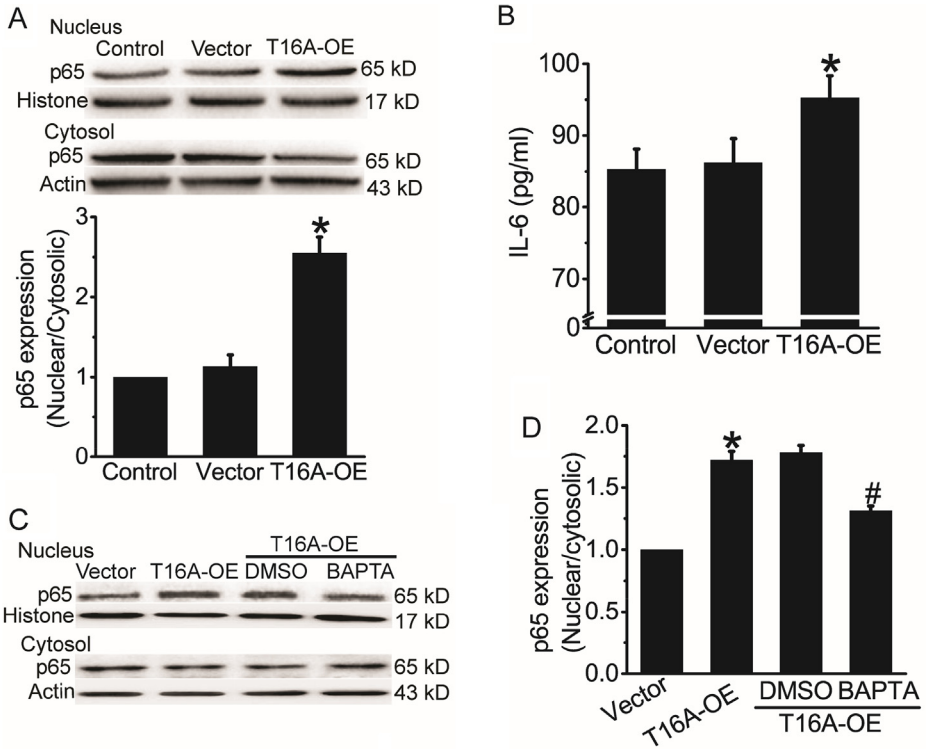

Fig. 4. TMEM16A overexpression activated NFκB signaling in AR42J cells. **A**. Western blot results of p65 expression in the nucleus and cytosol in control AR42J cells and cells transfected with empty vector or TMEM16A-overexpressing plasmids. Quantification results of the ratio of nuclear/cytosolic p65 expression in the bottom. n = 3 *p < 0.05 vs vector. **B**. ELISA results of the IL-6 levels in the culture medium in control AR42J cells and cells transfected with empty vector or TMEM16A-overexpressing plasmids. n = 6. *p < 0.05 vs vector. **C**. Representative Western blot results of p65 expression in the nucleus and cytosol in control AR42J cells and cells transfected with empty vector or TMEM16A-overexpressing plasmids in the presence or absence of BAPTA-AM (13 μM). DMSO was used as a vehicle control for BAPTA-AM. **D**. Quantification results of the ratio of nuclear/cytosolic p65 expression in C. n = 3. *p < 0.05 vs vector; #p < 0.05 vs DMSO.

IP_3R-mediated Ca^{2+} release induced by cerulein application (Fig. 3G, H). Taken together, these results suggested that TMEM16A and IP_3R directly interacted with and activated each other in AR42J cells.

TMEM16A overexpression activates NFκB signaling via Ca^{2+} in AR42J cells

Since NFκB activation by Ca^{2+} in PACs contributes to the pathogenesis of AP [25,27], we further investigated whether TMEM16A activates NFκB signaling in AR42J cells. TMEM16A overexpression increased the nuclear expression of NFκB/p65 and decreased the cytosolic expression of NFκB/p65 (Fig. 4A). TMEM16A overexpression also increased the IL-6 secretion from AR42J cells (Fig. 4B). These results suggested that TMEM16A promoted NFκB activation in AR42J cells. Furthermore, the Ca^{2+} chelator 1,2-bis(2-aminophenoxy)ethane-N,N,N′,N′-tetraacetic acid-acetyloxymethyl ester (BAPTA-AM) (Fig. S1C) inhibited TMEM16A overexpression-induced NFκB activation (Fig. 4C, D). These findings suggested that TMEM16A activated NFκB signaling by increasing intracellular Ca^{2+}.

TMEM16A knockdown blocks cerulein-induced NFκB activation

We next investigated the effect of TMEM16A inhibition on NFκB activation in the AR42J cell model of cerulein-induced AP. BAPTA-AM treatment inhibited cerulein-induced (24 h) NFκB activation (Fig. 5A), suggesting that Ca^{2+} signaling was critical for NFκB activation in cerulein-induced AP. Cerulein-induced NFκB activation and IL-6 secretion were inhibited by TMEM16A-shRNA treatment (Fig. 5B, C), suggesting that TMEM16A mediated NFκB activation and IL-6 secretion in cerulein-induced AP.

TMEM16A inhibitors ameliorate cerulein-induced AP via inhibition of channel activities and protein expression

We investigated the effect of TMEM16A inhibitors on NFκB activation in cerulein-induced AP. T16Ainh-A01 treatment inhibited cerulein-induced NFκB activation (Fig. 6A, B), suggesting that inhibition of TMEM16A channel function reduced the cerulein-induced NFκB activation in AR42J cells. To further confirm whether TMEM16A channel activities were essential for NFκB activation, we transfected AR42J cells with Δ_{444}EEEEEAVKD$_{452}$ TMEM16A mutants with reduced channel activities [28]. Compared with wild-type (WT) TMEM16A, overexpression of Δ_{444}EEEEEAVKD$_{452}$ mutants resulted in less NFκB activation (Fig. 6C), suggesting that TMEM16A channel activity was essential for NFκB activation.

We then examined whether T16Ainh-A01 inhibited TMEM16A expression in cerulein-treated AR42J cells. The cerulein-induced increase in TMEM16A expression was inhibited by T16Ainh-A01 treatment (Fig. 6D). This effect was also found in the *in vivo* mouse model of cerulein-induced AP (Fig. 6E). Furthermore, histological examination showed that T16Ainh-A01 reduced the pancreatic damage in AP mice (Fig. 6F, G). T16Ainh-A01 treatment inhibited the IL-6 level in the pancreatic tissues and the serum of AP mice (Fig. 6H, I). These findings indicated that TMEM16A inhibition ameliorated AP.

Discussion

Our study demonstrated that TMEM16A expression was upregulated in PACs via the IL-6/IL-6R/STAT3 signaling pathway in cerulein-induced AP, and increased TMEM16A expression activated NFκB signaling and promoted IL-6 secretion by increasing IP_3R-mediated Ca^{2+} release in acinar cells (Fig. 7). Thus, these

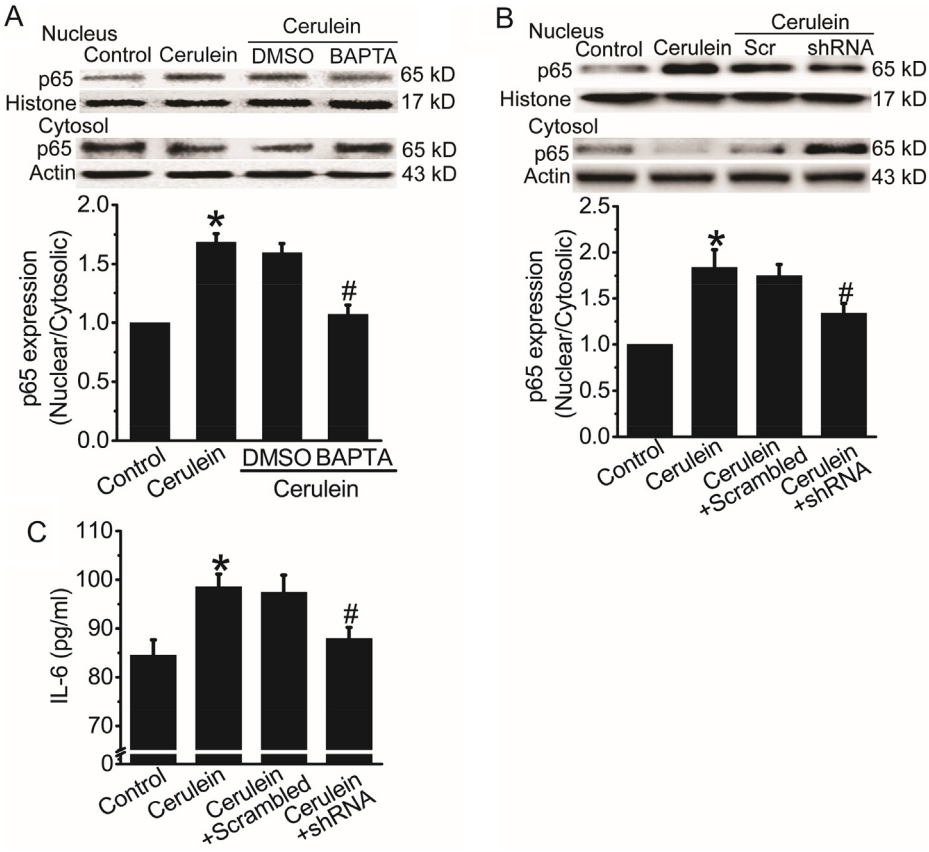

Fig. 5. TMEM16A inhibition blocked cerulein-induced NFκB activation in AR42J cells. **A**. Representative Western blot results (**Top**) of p65 expression in the nucleus and cytosol in control AR42J cells and cerulein-treated cells in the presence or absence of BAPTA-AM (13 μM). DMSO was used as vehicle control. **Bottom**: quantification results of the ratio of nuclear/cytosolic p65 expression. n = 3. *p < 0.05 vs control; #p < 0.05 vs DMSO. **B**. Western blot results (**Top**) of p65 expression in the nucleus and cytosol in control AR42J cells and cerulein-treated cells with or without transfection of scrambled shRNAs (Scr) or TMEM16A-shRNAs. **Bottom**: quantification results of the ratio of nuclear/cytosolic p65 expression. n = 3. *p < 0.05 vs control; #p < 0.05 vs scrambled shRNAs. **C**. ELISA results of the IL-6 levels in the culture medium in control AR42J cells and cerulein-treated cells with or without transfection of scrambled shRNAs or TMEM16A-shRNAs. n = 6. *p < 0.05 vs control; #p < 0.05 vs scrambled shRNAs.

results reveal a positive activation loop between TMEM16A and IL-6 in PACs. Since Ca^{2+}, NFκB, and IL-6 are known contributors to the pathogenesis of AP [20,27], our findings suggest that TMEM16A may aggravate AP by promoting Ca^{2+} elevation, NFκB activation and IL-6 release. Furthermore, TMEM16A inhibition by TMEM16A-shRNA or T16Ainh-A01 was able to block NFκB activation and IL-6 secretion in the cellular model of AP, and T16inh-A01 treatment ameliorated pancreatic damage and reduced the IL-6 levels in the AP animal model. Our findings suggest that TMEM16A inhibition may be a new strategy for treating AP.

TMEM16A expression is upregulated in inflammation [10], and TMEM16A overexpression contributes to inflammation-associated respiratory diseases such as cystic fibrosis, chronic rhinosinusitis, and asthma [8,9,11]. Inflammatory cytokines such as IL-4 and IL-13 increase TMEM16A expression by activating STAT6 in airway epithelial cells and biliary epithelial cells [10,29,30]. We previously found that TMEM16A expression is upregulated by epidermal growth factor (EGF)/EGF receptor (EGFR)/STAT3 signaling activation in breast cancer cells [31]. The current study showed that TMEM16A expression was correlated with the IL-6 levels in the pancreatic tissues and in the serum of AP mice, and IL-6 promoted TMEM16A expression in PACs by activating the IL-6R/STAT3 signaling pathway. Furthermore, TMEM16A overexpression resulted in an increase in IL-6 secretion in PACs, and TMEM16A knockdown reduced IL-6 secretion in cerulein-treated cells. These findings suggest that TMEM16A expression and IL-6 secretion mutually activate each other in PACs, and the positive activation loop between TMEM16A and IL-6 may be important for the maintenance of persistent high TMEM16A expression and the constitutive secretion of IL-6 in PACs during AP. Since IL-6 is a pro-inflammatory cytokine that contributes to the development of AP [25], our findings also suggest that TMEM16A upregulation in PACs may promote AP by increasing IL-6 secretion.

Sustained Ca^{2+} elevation is an early cellular event in PACs during AP [3,20,27]. NFκB activation and the subsequent release of many pro-inflammatory cytokines including IL-6 play key roles in the pathogenesis of AP [25,27]. Several studies have demonstrated that Ca^{2+} is required for NFκB activation in PACs treated with cerulein or bile acids [27,32]. Consistent with these studies, we found that the Ca^{2+} chelator BAPTA-AM reduced cerulein-induced NFκB activation in PACs. In addition, TMEM16A inhibition by T16Ainh-A01 reduced the IP_3R-mediated Ca^{2+} release induced by cerulein, and BAPTA-AM treatment inhibited the TMEM16A overexpression-induced NFκB activation in PACs. Thus, TMEM16A overexpression activates NFκB by increasing Ca^{2+} levels. Furthermore, TMEM16A inhibition by shRNAs or T16Ainh-A01 reduced the cerulein-induced NFκB activation. Therefore, our findings suggest that TMEM16A may promote AP by increasing intracellular Ca^{2+} concentrations and subsequently activating NFκB in PACs.

TMEM16A is expressed in the ER–plasma membrane contact sites [21,22], where ion channels such as IP_3R are expressed and participate in the regulation of Ca^{2+} signaling [33]. TMEM16A directly binds to IP_3R and is activated by IP_3R-mediated Ca^{2+} release in the dorsal root ganglia and HeLa cells [21,22]. Furthermore, TMEM16A knockdown inhibits ATP-induced Ca^{2+} release in HeLa cells and human cystic fibrosis bronchial epithelial (CFBE)

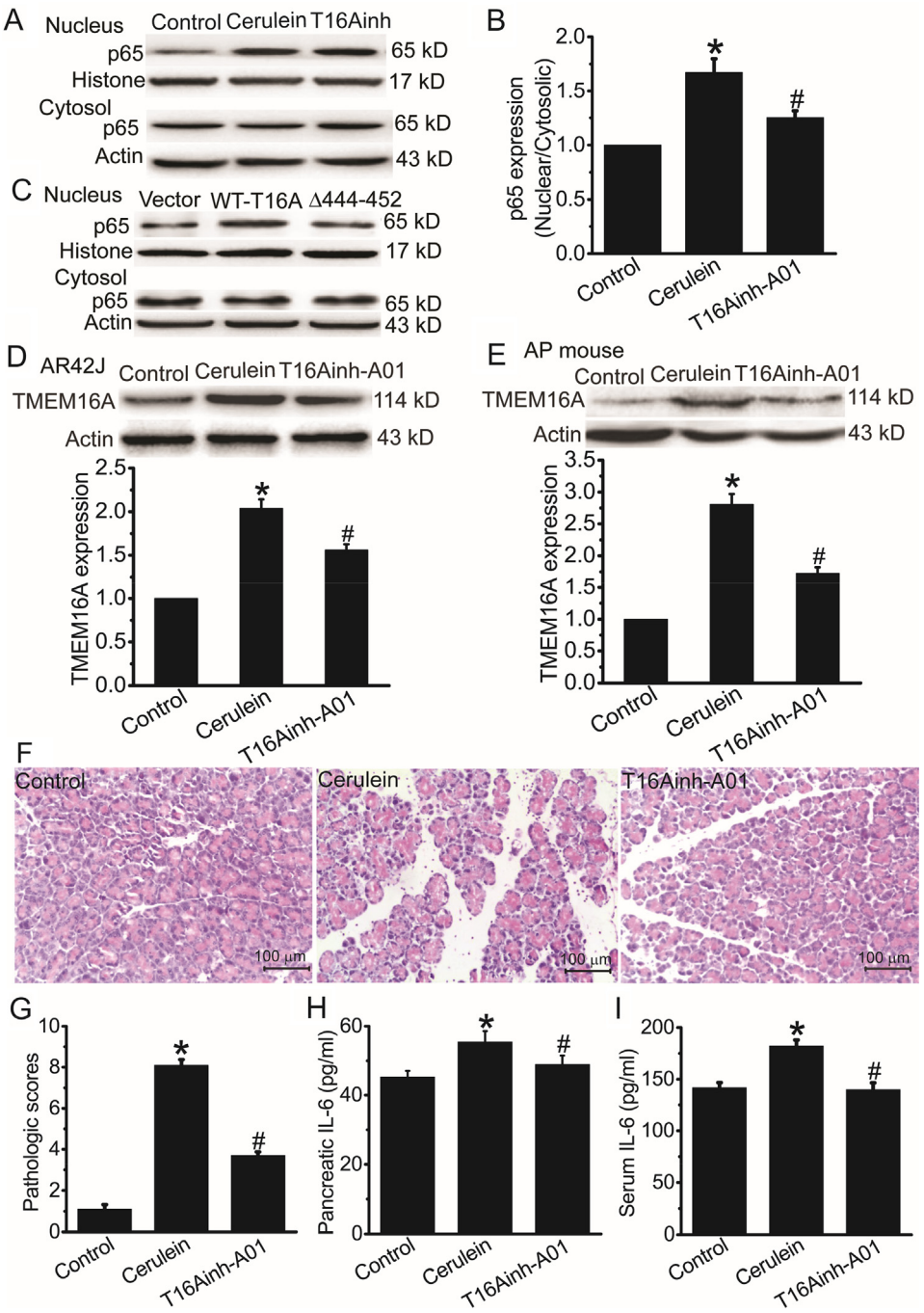

Fig. 6. T16Ainh-A01 inhibited cerulein-induced AP. **A**. Representative Western blot results of p65 expression in the nucleus and cytosol in control AR42J cells and cerulein-treated cells in the presence or absence of T16Ainh-A01 treatment applied 30 min before cerulein treatment. **B**. Quantification results of the ratio of nuclear/cytosolic p65 expression in (**A**). n = 3. *p < 0.05 vs control; #p < 0.05 vs cerulein alone. **C**. Western blot results of p65 expression in the nucleus and cytosol in AR42J cells transfected with empty vector, WT TMEM16A, or Δ_{444}EEEEAVKD$_{452}$ TMEM16A mutants. **D. E.** Western blot results (**Top**) of TMEM16A expression in control AR42J cells, cerulein-treated cells (**D**), control mice and mice with cerulein treatment (**E**) in the presence or absence of T16Ainh-A01. **Bottom**: quantification results of TMEM16A expression. n = 3. *p < 0.05 vs control; #p < 0.05 vs cerulein alone. **F. G**. Representative H&E stains (**F**) and pathological scores (**G**) of pancreatic tissues in control mice and mice with cerulein treatment in the presence or absence of T16Ainh-A01. **H. I**. The IL-6 levels in the pancreatic tissues (**H**) and in the serum (**I**) of control mice and mice with cerulein treatment in the presence or absence of T16Ainh-A01. n = 6. *p < 0.05 vs control; #p < 0.05 vs cerulein alone.

cells [22,34]. However, the binding of TMEM16A to IP_3R is cell type-dependent, since TMEM16A does not co-immunoprecipitate with IP_3R in cerebral artery smooth muscles [23]. In addition, TMEM16A has been found to control EGF-induced Ca^{2+} signaling in pancreatic cancer cells [17]. Here, we found that TMEM16A and IP_3R were co-immunoprecipitated in PACs. TMEM16A channels were activated by Ca^{2+} release from IP_3R activation by cerulein. In turn, TMME16A inhibition by T16Ainh-A01 reduced IP_3R-mediated Ca^{2+} release. These results demonstrate that IP_3R-mediated Ca^{2+} release can activate TMEM16A channels, and TMEM16A channels can promote IP_3R-mediated Ca^{2+} release from the ER. Thus, our findings suggest that TMEM16A and IP_3R directly interact with and activate each other, thus forming a positive activation loop between TMEM16A and IP_3R.

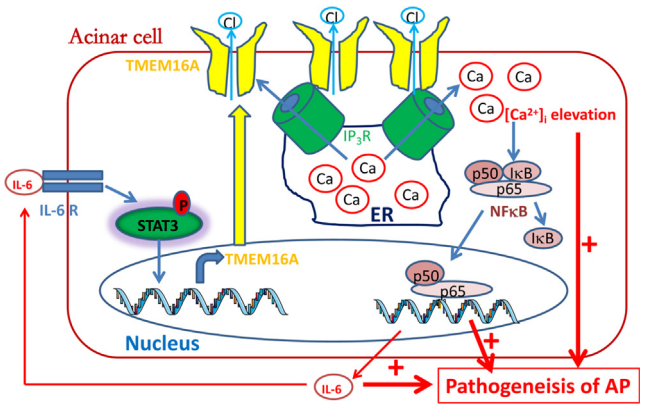

Fig. 7. The mechanisms by which TMEM16A promotes the pathogenesis of AP by activating the IP_3R/Ca^{2+}/NFκB signaling pathways. TMEM16A is upregulated by IL-6 via the IL-6R/STAT3 signaling pathway. Increased TMEM16A expression promotes intracellular Ca^{2+} release from the ER via direct interaction with IP_3R. Intracellular Ca^{2+} elevation subsequently activates NFκB signaling, resulting in an increase in IL-6 secretion from acinar cells. IL-6 further promotes TMEM16A expression via the IL-6R/STAT3 signaling pathway. Therefore, a positive activation loop between TMEM16A and the IP_3R/ Ca^{2+}/NFκB/IL-6 pathway is important for Ca^{2+} elevation, NFκB activation and IL-6 release, and thus cooperatively promotes the pathogenesis of AP.

IP_3R-mediated Ca^{2+} elevation in PACs is important for the pathogenesis of AP [20], since IP_3R inhibition by IP_3R knockout and by the pharmacological inhibitor caffeine protects against AP induced by cerulein, taurolithocholate, or ethanol and palmitoleic acid [35]. However, caffeine is not a specific IP_3R inhibitor, and intoxication doses (>25 mg/kg) are required to ameliorate AP in mice [35]. This study found that TMEM16A inhibition by T16Ainh-A01 inhibited the IP_3R-mediated Ca^{2+} elevation and cerulein-induced NFκB activation in the AR42J cell model of AP, and it reduced the serum IL-6 levels and ameliorated pancreatic damage in the animal model of AP. Our findings indicate that TMEM16A may be a potential new target for treating AP.

We found that TMEM16A expression was upregulated in PACs, and reduced TMEM16A expression via transfection of TMEM16A-shRNAs inhibited the cerulein-induced NFκB activation, suggesting that reduced TMEM16A channel function via decreasing protein levels is important for NFκB activation in PACs. However, knockdown of TMEM16A protein could not determine whether TMEM16A channel activity contributes to NFκB activation. Our findings show that overexpression of Δ_{444}EEEEEAVKD$_{452}$ mutants with decreased channel activities resulted in less NFκB activation, suggesting that TMEM16A channel activity is important for NFκB activation in AR42J cells. Furthermore, T16Ainh-A01 not only inhibited the TMEM16A current activated by cerulein, but it also reduced TMEM16A expression in cell and mouse models of cerulein-induced AP. Reduced TMEM16A protein expression is found for CaCCinh-A01 (but not for T16Ainh-A01) in head and neck squamous cell carcinoma Te11 cells and in pharyngeal squamous cancer FaDu cells due to decreased protein stability or increased internalization via an ER-associated, proteasome-dependent mechanism [36]. However, T16Ainh-A01 has been found to reduce TMEM16 expression in SKBR3 breast cancer cells [37], similar to our findings. This cell-specific effect of T16Ainh-A01 on TMEM16A expression suggests that the reduction of TMEM16A expression by T16Ainh-A01 may depend on a specific cellular environment. In this study, T16Ainh-A01 inhibited NFκB activation by cerulein in AR42J cells, and reduced the IL-6 levels in the pancreatic tissues and serum. Since IL-6 promoted TMEM16A expression (Fig. 7), the reduction of TMEM16A expression by T16Ainh-A01 may be due to reduced IL-6 levels via NFκB inhibition in PACs.

Conclusions

Our study identified a novel mechanism by which TMEM16A channels are upregulated in PACs via IL-6/IL-6R/STAT3 signaling activation, and TMEM16A overexpression activates IP_3R/Ca^{2+}/NFκB/IL-6 signaling in PACs (Fig. 7). The mutual activation between TMEM16A and IL-6 may be essential for persistent high TMEM16A expression, sustained Ca^{2+} elevation, and constitutive NFκB activation and IL-6 secretion in PACs, all of which are known to contribute to the pathogenesis of AP. Furthermore, TMEM16A inhibition by T16Ainh-A01 reduced the serum IL-6 levels and ameliorated pancreatic damage in AP mice. Therefore, our findings suggest that targeting TMEM16A may represent a novel therapy for AP. The identification of novel TMEM16A inhibitors may be promising for the treatment of AP. Consistent with this idea, some agents such as sikonin that inhibit TMEM16A [38] can ameliorate AP in mice [39].

Compliance with ethics requirements

All Institutional and National Guidelines for the care and use of animals (fisheries) were followed.

Declaration of Competing Interest

All authors declare no conflicts of interest.

Acknowledgements

This work was supported by grants from the National Natural Science Foundation of China (No. 81572613 and No. 31371145 to Qinghuan Xiao; No. 81702611 to Hui Wang), the Liaoning Pandeng Scholar (to Qinghuan Xiao), the Natural Science Foundation of Liaoning Province (No. 2019-MS-222 to Qinghua Wang), and the Natural Science Foundation of Liaoning Province for Guidance Program (No. 20180551125 to Lichuan Bai).

Appendix A. Supplementary material

Supplementary data to this article can be found online at https://doi.org/10.1016/j.jare.2020.01.006.

References

[1] Goodchild G, Chouhan M, Johnson GJ. Practical guide to the management of acute pancreatitis. Frontline Gastroenterol 2019;10:292–9. doi: https://doi.org/10.1136/flgastro-2018-101102.
[2] Roberts SE, Akbari A, Thorne K, Atkinson M, Evans PA. The incidence of acute pancreatitis: impact of social deprivation, alcohol consumption, seasonal and demographic factors. Aliment Pharmacol Ther 2013;38:539–48. doi: https://doi.org/10.1111/apt.12408.
[3] Habtezion A, Gukovskaya AS, Pandol SJ. Acute pancreatitis: a multifaceted set of organelle and cellular interactions. Gastroenterology 2019;156:1941–50. doi: https://doi.org/10.1053/j.gastro.2018.11.082.
[4] Oh U, Jung J. Cellular functions of TMEM16/anoctamin. Pflugers Arch 2016;468:443–53. doi: https://doi.org/10.1007/s00424-016-1790-0.
[5] Dayal A, Ng SFJ, Grabner M. Ca(2+)-activated Cl(-) channel TMEM16A/ANO1 identified in zebrafish skeletal muscle is crucial for action potential acceleration. Nat Commun 2019;10:115. doi: https://doi.org/10.1038/s41467-018-07918-z.
[6] Ma MM, Gao M, Guo KM, Wang M, Li XY, Zeng XL, et al. TMEM16A contributes to endothelial dysfunction by facilitating Nox2 NADPH oxidase-derived reactive oxygen species generation in hypertension. Hypertension 2017;69:892–901. doi: https://doi.org/10.1161/HYPERTENSIONAHA.116.08874.
[7] Wang H, Zou L, Ma K, Yu J, Wu H, Wei M, et al. Cell-specific mechanisms of TMEM16A Ca(2+)-activated chloride channel in cancer. Mol Cancer 2017;16:152. doi: https://doi.org/10.1186/s12943-017-0720-x.
[8] Kunzelmann K, Ousingsawat J, Cabrita I, Dousova T, Bahr A, Janda M, et al. TMEM16A in cystic fibrosis: activating or inhibiting?. Front Pharmacol 2019;10:3. doi: https://doi.org/10.3389/fphar.2019.00003.

[9] Wang P, Zhao W, Sun J, Tao T, Chen X, Zheng YY, et al. Inflammatory mediators mediate airway smooth muscle contraction through a G protein-coupled receptor-transmembrane protein 16A-voltage-dependent Ca(2+) channel axis and contribute to bronchial hyperresponsiveness in asthma e1211. J Allergy Clin Immunol 2018;141:1259–68. doi: https://doi.org/10.1016/j.jaci.2017.05.053.
[10] Caputo A, Caci E, Ferrera L, Pedemonte N, Barsanti C, Sondo E, et al. TMEM16A, a membrane protein associated with calcium-dependent chloride channel activity. Science 2008;322:590–4. doi: https://doi.org/10.1126/science.1163518.
[11] Zhang Y, Wang X, Wang H, Jiao J, Li Y, Fan E, et al. TMEM16A-mediated mucin secretion in IL-13-induced nasal epithelial cells from chronic rhinosinusitis patients. Allergy Asthma Immunol Res 2015;7:367–75. doi: https://doi.org/10.4168/aair.2015.7.4.367.
[12] Yang YD, Cho H, Koo JY, Tak MH, Cho Y, Shim WS, et al. TMEM16A confers receptor-activated calcium-dependent chloride conductance. Nature 2008;455:1210–5. doi: https://doi.org/10.1038/nature07313.
[13] Yokoyama T, Takemoto M, Hirakawa M, Saino T. Different immunohistochemical localization for TMEM16A and CFTR in acinar and ductal cells of rat major salivary glands and exocrine pancreas. Acta Histochem 2019;121:50–5. doi: https://doi.org/10.1016/j.acthis.2018.10.013.
[14] Huang F, Rock JR, Harfe BD, Cheng T, Huang X, Jan YN, et al. Studies on expression and function of the TMEM16A calcium-activated chloride channel. Proc Natl Acad Sci USA 2009;106:21413–8. doi: https://doi.org/10.1073/pnas.0911935106.
[15] Crutzen R, Virreira M, Markadieu N, Shlyonsky V, Sener A, Malaisse WJ, et al. Anoctamin 1 (Ano1) is required for glucose-induced membrane potential oscillations and insulin secretion by murine beta-cells. Pflugers Arch 2016;468:573–91. doi: https://doi.org/10.1007/s00424-015-1758-5.
[16] Wang J, Haanes KA, Novak I. Purinergic regulation of CFTR and Ca(2+)-activated Cl(-) channels and K(+) channels in human pancreatic duct epithelium. Am J Physiol Cell Physiol 2013;304:C673–84. doi: https://doi.org/10.1152/ajpcell.00196.2012.
[17] Crottes D, Lin YT, Peters CJ, Gilchrist JM, Wiita AP, Jan YN, et al. TMEM16A controls EGF-induced calcium signaling implicated in pancreatic cancer prognosis. Proc Natl Acad Sci USA 2019;116:13026–35. doi: https://doi.org/10.1073/pnas.1900703116.
[18] Ousingsawat J, Martins JR, Schreiber R, Rock JR, Harfe BD, Kunzelmann K. Loss of TMEM16A causes a defect in epithelial Ca2+-dependent chloride transport. J Biol Chem 2009;284:28698–703. doi: https://doi.org/10.1074/jbc.M109.012120.
[19] Han Y, Shewan AM, Thorn P. HCO3-transport through anoctamin/transmembrane protein ANO1/TMEM16A in pancreatic acinar cells regulates luminal pH. J Biol Chem 2016;291:20345–52. doi: https://doi.org/10.1074/jbc.M116.750224.
[20] Gerasimenko JV, Peng S, Tsugorka T, Gerasimenko OV. Ca(2+) signalling underlying pancreatitis. Cell Calcium 2018;70:95–101. doi: https://doi.org/10.1016/j.ceca.2017.05.010.
[21] Jin X, Shah S, Liu Y, Zhang H, Lees M, Fu Z, et al. Activation of the Cl- channel ANO1 by localized calcium signals in nociceptive sensory neurons requires coupling with the IP3 receptor. Sci Signal 2013;6:ra73. doi: https://doi.org/10.1126/scisignal.2004184.
[22] Cabrita I, Benedetto R, Fonseca A, Wanitchakool P, Sirianant L, Skryabin BV, et al. Differential effects of anoctamins on intracellular calcium signals. FASEB J 2017;31:2123–34. doi: https://doi.org/10.1096/fj.201600797RR.
[23] Wang Q, Leo MD, Narayanan D, Kuruvilla KP, Jaggar JH. Local coupling of TRPC6 to ANO1/TMEM16A channels in smooth muscle cells amplifies vasoconstriction in cerebral arteries. Am J Physiol Cell Physiol 2016;310:C1001–9. doi: https://doi.org/10.1152/ajpcell.00092.2016.
[24] Wang Y, Kayoumu A, Lu G, Xu P, Qiu X, Chen L, et al. Experimental models in syrian golden hamster replicate human acute pancreatitis. Sci Rep 2016;6:28014. doi: https://doi.org/10.1038/srep28014.
[25] Manohar M, Verma AK, Venkateshaiah SU, Sanders NL, Mishra A. Pathogenic mechanisms of pancreatitis. World J Gastrointest Pharmacol Ther 2017;8:10–25. doi: https://doi.org/10.4292/wjgpt.v8.i1.10.
[26] Suzuki S, Miyasaka K, Jimi A, Funakoshi A. Induction of acute pancreatitis by cerulein in human IL-6 gene transgenic mice. Pancreas 2000;21:86–92.
[27] Jakkampudi A, Jangala R, Reddy BR, Mitnala S, Nageshwar Reddy D, Talukdar R. NF-kappaB in acute pancreatitis: Mechanisms and therapeutic potential. Pancreatology 2016;16:477–88. doi: https://doi.org/10.1016/j.pan.2016.05.001.
[28] Xiao Q, Cui Y. Acidic amino acids in the first intracellular loop contribute to voltage- and calcium- dependent gating of anoctamin1/TMEM16A. PLoS ONE 2014;9:e99376. doi: https://doi.org/10.1371/journal.pone.0099376.
[29] Qin Y, Jiang Y, Sheikh AS, Shen S, Liu J, Jiang D. Interleukin-13 stimulates MUC5AC expression via a STAT6-TMEM16A-ERK1/2 pathway in human airway epithelial cells. Int Immunopharmacol 2016;40:106–14. doi: https://doi.org/10.1016/j.intimp.2016.08.033.
[30] Dutta AK, Khimji AK, Kresge C, Bugde A, Dougherty M, Esser V, et al. Identification and functional characterization of TMEM16A, a Ca2+-activated Cl- channel activated by extracellular nucleotides, in biliary epithelium. J Biol Chem 2011;286:766–76. doi: https://doi.org/10.1074/jbc.M110.164970.
[31] Wang H, Yao F, Luo S, Ma K, Liu M, Bai L, et al. A mutual activation loop between the Ca(2+)-activated chloride channel TMEM16A and EGFR/STAT3 signaling promotes breast cancer tumorigenesis. Cancer Lett 2019;455:48–59. doi: https://doi.org/10.1016/j.canlet.2019.04.027.
[32] Muili KA, Jin S, Orabi AI, Eisses JF, Javed TA, Le T, et al. Pancreatic acinar cell nuclear factor kappaB activation because of bile acid exposure is dependent on calcineurin. J Biol Chem 2013;288:21065–73. doi: https://doi.org/10.1074/jbc.M113.471425.
[33] Chung WY, Jha A, Ahuja M, Muallem S. Ca(2+) influx at the ER/PM junctions. Cell Calcium 2017;63:29–32. doi: https://doi.org/10.1016/j.ceca.2017.02.009.
[34] Benedetto R, Ousingsawat J, Wanitchakool P, Zhang Y, Holtzman MJ, Amaral M, et al. Epithelial chloride transport by CFTR requires TMEM16A. Sci Rep 2017;7:12397. doi: https://doi.org/10.1038/s41598-017-10910-0.
[35] Huang W, Cane MC, Mukherjee R, Szatmary P, Zhang X, Elliott V, et al. Caffeine protects against experimental acute pancreatitis by inhibition of inositol 1,4,5-trisphosphate receptor-mediated Ca2+ release. Gut 2017;66:301–13. doi: https://doi.org/10.1136/gutjnl-2015-309363.
[36] Bill A, Hall ML, Borawski J, Hodgson C, Jenkins J, Piechon P, et al. Small molecule-facilitated degradation of ANO1 protein: a new targeting approach for anticancer therapeutics. J Biol Chem 2014;289:11029–41. doi: https://doi.org/10.1074/jbc.M114.549188.
[37] Kulkarni S, Bill A, Godse NR, Khan NI, Kass JI, Steehler K, et al. TMEM16A/ANO1 suppression improves response to antibody-mediated targeted therapy of EGFR and HER2/ERBB2. Genes Chromosom Cancer 2017;56:460–71. doi: https://doi.org/10.1002/gcc.22450.
[38] Jiang Y, Yu B, Yang H, Ma T. Shikonin inhibits intestinal calcium-activated chloride channels and prevents rotaviral diarrhea. Front Pharmacol 2016;7:270. doi: https://doi.org/10.3389/fphar.2016.00270.
[39] Xiong J, Ni J, Hu G, Shen J, Zhao Y, Yang L, et al. Shikonin ameliorates cerulein-induced acute pancreatitis in mice. J Ethnopharmacol 2013;145:573–80. doi: https://doi.org/10.1016/j.jep.2012.11.032.